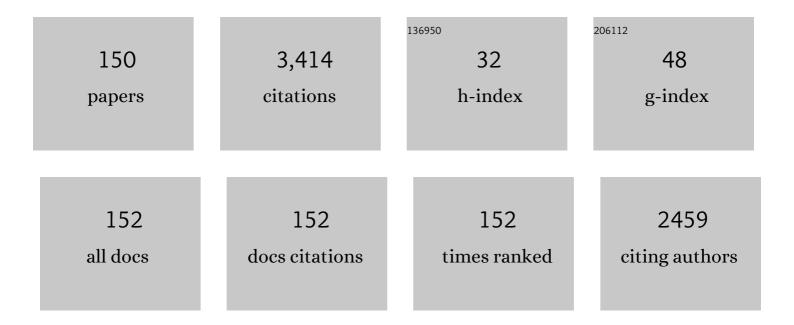
Claudia Prieto

List of Publications by Year in descending order

Source: https://exaly.com/author-pdf/9384732/publications.pdf Version: 2024-02-01



#	Article	IF	CITATIONS
1	Motion corrected compressed sensing for freeâ€breathing dynamic cardiac MRI. Magnetic Resonance in Medicine, 2013, 70, 504-516.	3.0	142
2	Wholeâ€heart coronary MR angiography with 2D selfâ€navigated image reconstruction. Magnetic Resonance in Medicine, 2012, 67, 437-445.	3.0	135
3	CINENet: deep learning-based 3D cardiac CINE MRI reconstruction with multi-coil complex-valued 4D spatio-temporal convolutions. Scientific Reports, 2020, 10, 13710.	3.3	122
4	Highly efficient respiratory motion compensated freeâ€breathing coronary mra using goldenâ€step Cartesian acquisition. Journal of Magnetic Resonance Imaging, 2015, 41, 738-746.	3.4	121
5	Highly efficient nonrigid motionâ€corrected 3D wholeâ€heart coronary vessel wall imaging. Magnetic Resonance in Medicine, 2017, 77, 1894-1908.	3.0	85
6	From Compressed-Sensing to Artificial Intelligence-Based Cardiac MRI Reconstruction. Frontiers in Cardiovascular Medicine, 2020, 7, 17.	2.4	85
7	Highâ€dimensionality undersampled patchâ€based reconstruction (HDâ€PROST) for accelerated multiâ€contrast MRI. Magnetic Resonance in Medicine, 2019, 81, 3705-3719.	3.0	79
8	kâ€ŧ group sparse: A method for accelerating dynamic MRI. Magnetic Resonance in Medicine, 2011, 66, 1163-1176.	3.0	78
9	Fiveâ€minute wholeâ€heart coronary MRA with subâ€millimeter isotropic resolution, 100% respiratory scan efficiency, and 3Dâ€PROST reconstruction. Magnetic Resonance in Medicine, 2019, 81, 102-115.	3.0	73
10	Automatic CNN-based detection of cardiac MR motion artefacts using k-space data augmentation and curriculum learning. Medical Image Analysis, 2019, 55, 136-147.	11.6	71
11	Accelerated motion corrected threeâ€dimensional abdominal MRI using total variation regularized SENSE reconstruction. Magnetic Resonance in Medicine, 2016, 75, 1484-1498.	3.0	69
12	Nonrigid Motion Modeling of the Liver From 3-D Undersampled Self-Gated Golden-Radial Phase Encoded MRI. IEEE Transactions on Medical Imaging, 2012, 31, 805-815.	8.9	55
13	PET image reconstruction using multi-parametric anato-functional priors. Physics in Medicine and Biology, 2017, 62, 5975-6007.	3.0	54
14	Free breathing whole-heart 3D CINE MRI with self-gated Cartesian trajectory. Magnetic Resonance Imaging, 2017, 38, 129-137.	1.8	53
15	Multiâ€parametric liver tissue characterization using MR fingerprinting: Simultaneous T ₁ , T ₂ , T ₂ *, and fat fraction mapping. Magnetic Resonance in Medicine, 2020, 84, 2625-2635.	3.0	50
16	Deep Learning-Based Detection and Correction of Cardiac MR Motion Artefacts During Reconstruction for High-Quality Segmentation. IEEE Transactions on Medical Imaging, 2020, 39, 4001-4010.	8.9	49
17	Water–fat Dixon cardiac magnetic resonance fingerprinting. Magnetic Resonance in Medicine, 2020, 83, 2107-2123.	3.0	48
18	3D undersampled goldenâ€radial phase encoding for DCEâ€MRA using inherently regularized iterative SENSE. Magnetic Resonance in Medicine. 2010. 64. 514-526.	3.0	47

#	Article	IF	CITATIONS
19	Sparsity and locally low rank regularization for MR fingerprinting. Magnetic Resonance in Medicine, 2019, 81, 3530-3543.	3.0	46
20	Accelerated cardiac cine MRI using locally low rank and finite difference constraints. Magnetic Resonance Imaging, 2016, 34, 707-714.	1.8	43
21	Wholeâ€Heart Coronary <scp>MRA</scp> with 3D Affine Motion Correction Using 3D Imageâ€Based Navigation. Magnetic Resonance in Medicine, 2014, 71, 173-181.	3.0	42
22	Motion orrected simultaneous cardiac positron emission tomography and coronary MR angiography with high acquisition efficiency. Magnetic Resonance in Medicine, 2018, 79, 339-350.	3.0	42
23	MR-Based Cardiac and Respiratory Motion-Compensation Techniques for PET-MR Imaging. PET Clinics, 2016, 11, 179-191.	3.0	40
24	Improved UTE-based attenuation correction for cranial PET-MR using dynamic magnetic field monitoring. Medical Physics, 2013, 41, 012302.	3.0	39
25	100% Efficient threeâ€dimensional coronary MR angiography with twoâ€dimensional beatâ€toâ€beat translational and binâ€toâ€bin affine motion correction. Magnetic Resonance in Medicine, 2015, 74, 756-764.	3.0	38
26	Free-running cardiac magnetic resonance fingerprinting: Joint T1/T2 map and Cine imaging. Magnetic Resonance Imaging, 2020, 68, 173-182.	1.8	38
27	Rigid motionâ€corrected magnetic resonance fingerprinting. Magnetic Resonance in Medicine, 2019, 81, 947-961.	3.0	37
28	3D freeâ€breathing cardiac magnetic resonance fingerprinting. NMR in Biomedicine, 2020, 33, e4370.	2.8	37
29	3D whole-heart isotropic sub-millimeter resolution coronary magnetic resonance angiography with non-rigid motion-compensated PROST. Journal of Cardiovascular Magnetic Resonance, 2020, 22, 24.	3.3	37
30	Modelâ€based reconstruction for cardiac cine MRI without ECG or breath holding. Magnetic Resonance in Medicine, 2010, 63, 1247-1257.	3.0	36
31	Freeâ€running 3D whole heart myocardial T 1 mapping with isotropic spatial resolution. Magnetic Resonance in Medicine, 2019, 82, 1331-1342.	3.0	36
32	Manifold learning based ECGâ€free freeâ€breathing cardiac CINE MRI. Journal of Magnetic Resonance Imaging, 2015, 41, 1521-1527.	3.4	35
33	Synergistic PET and SENSE MR Image Reconstruction Using Joint Sparsity Regularization. IEEE Transactions on Medical Imaging, 2018, 37, 20-34.	8.9	35
34	SIRF: Synergistic Image Reconstruction Framework. Computer Physics Communications, 2020, 249, 107087.	7.5	35
35	A 3D MRâ€acquisition scheme for nonrigid bulk motion correction in simultaneous PETâ€MR. Medical Physics, 2014, 41, 082304.	3.0	33
36	Simultaneous bright―and blackâ€blood wholeâ€heart MRI for noncontrast enhanced coronary lumen and thrombus visualization. Magnetic Resonance in Medicine, 2018, 79, 1460-1472.	3.0	33

#	Article	IF	CITATIONS
37	Non-Rigid Respiratory Motion Estimation of Whole-Heart Coronary MR Images Using Unsupervised Deep Learning. IEEE Transactions on Medical Imaging, 2021, 40, 444-454.	8.9	33
38	Retrospective Rigid Motion Correction in k-Space for Segmented Radial MRI. IEEE Transactions on Medical Imaging, 2014, 33, 1-10.	8.9	32
39	3D whole-heart phase sensitive inversion recovery CMR for simultaneous black-blood late gadolinium enhancement and bright-blood coronary CMR angiography. Journal of Cardiovascular Magnetic Resonance, 2016, 19, 94.	3.3	32
40	A multi-scale variational neural network for accelerating motion-compensated whole-heart 3D coronary MR angiography. Magnetic Resonance Imaging, 2020, 70, 155-167.	1.8	32
41	Deepâ€learning based superâ€resolution for 3D isotropic coronary MR angiography in less than a minute. Magnetic Resonance in Medicine, 2021, 86, 2837-2852.	3.0	32
42	Free-running simultaneous myocardial T1/T2 mapping and cine imaging with 3D whole-heart coverage and isotropic spatial resolution. Magnetic Resonance Imaging, 2019, 63, 159-169.	1.8	29
43	Clinical comparison of sub-mm high-resolution non-contrast coronary CMR angiography against coronary CT angiography in patients with low-intermediate risk of coronary artery disease: a single center trial. Journal of Cardiovascular Magnetic Resonance, 2021, 23, 57.	3.3	28
44	Optimized respiratoryâ€resolved motionâ€compensated 3 <scp>D C</scp> artesian coronary <scp>MR</scp> angiography. Magnetic Resonance in Medicine, 2018, 80, 2618-2629.	3.0	27
45	Motion-corrected whole-heart PET-MR for the simultaneous visualisation of coronary artery integrity and myocardial viability: an initial clinical validation. European Journal of Nuclear Medicine and Molecular Imaging, 2018, 45, 1975-1986.	6.4	27
46	<scp>T1</scp> , <scp>T2,</scp> and Fat Fraction Cardiac MR Fingerprinting: Preliminary Clinical Evaluation. Journal of Magnetic Resonance Imaging, 2021, 53, 1253-1265.	3.4	27
47	Wholeâ€heart imaging using undersampled radial phase encoding (RPE) and iterative sensitivity encoding (SENSE) reconstruction. Magnetic Resonance in Medicine, 2009, 62, 1331-1337.	3.0	25
48	Coronary Magnetic Resonance Angiography. JACC: Cardiovascular Imaging, 2020, 13, 2653-2672.	5.3	25
49	Motion-corrected 3D whole-heart water-fat high-resolution late gadolinium enhancement cardiovascular magnetic resonance imaging. Journal of Cardiovascular Magnetic Resonance, 2020, 22, 53.	3.3	24
50	Highly efficient 3D motion-compensated abdomen MRI from undersampled golden-RPE acquisitions. Magnetic Resonance Materials in Physics, Biology, and Medicine, 2013, 26, 419-429.	2.0	23
51	3D wholeâ€heart isotropicâ€resolution motionâ€compensated joint T ₁ /T ₂ mapping and water/fat imaging. Magnetic Resonance in Medicine, 2020, 84, 3009-3026.	3.0	23
52	Respiratory motion-compensated high-resolution 3D whole-heart T1ï•mapping. Journal of Cardiovascular Magnetic Resonance, 2020, 22, 12.	3.3	23
53	Generalized lowâ€rank nonrigid motionâ€corrected reconstruction for MR fingerprinting. Magnetic Resonance in Medicine, 2022, 87, 746-763.	3.0	22
54	Endâ€ŧoâ€end deep learning nonrigid motion orrected reconstruction for highly accelerated freeâ€breathing coronary MRA. Magnetic Resonance in Medicine, 2021, 86, 1983-1996.	3.0	21

Claudia Prieto

#	Article	IF	CITATIONS
55	Complementary timeâ€frequency domain networks for dynamic parallel MR image reconstruction. Magnetic Resonance in Medicine, 2021, 86, 3274-3291.	3.0	21
56	Simultaneous T ₁ , T ₂ , and T _{1Ï} cardiac magnetic resonance fingerprinting for contrast agent–free myocardial tissue characterization. Magnetic Resonance in Medicine, 2022, 87, 1992-2002.	3.0	21
57	Myocardial T1, T2, T2*, and fat fraction quantification via lowâ€rank motionâ€corrected cardiac MR fingerprinting. Magnetic Resonance in Medicine, 2022, 87, 2757-2774.	3.0	21
58	Reconstruction of undersampled dynamic images by modeling the motion of object elements. Magnetic Resonance in Medicine, 2007, 57, 939-949.	3.0	20
59	Cardiac Magnetic Resonance Fingerprinting: Technical Developments and Initial Clinical Validation. Current Cardiology Reports, 2019, 21, 91.	2.9	20
60	Nonâ€contrast enhanced simultaneous 3D wholeâ€heart brightâ€blood pulmonary veins visualization and blackâ€blood quantification of atrial wall thickness. Magnetic Resonance in Medicine, 2019, 81, 1066-1079.	3.0	20
61	Isotropic 3D Cartesian single breathâ€hold CINE MRI with multiâ€bin patchâ€based lowâ€rank reconstruction. Magnetic Resonance in Medicine, 2020, 84, 2018-2033.	3.0	20
62	A Survey on Deep Learning and Explainability for Automatic Report Generation from Medical Images. ACM Computing Surveys, 2022, 54, 1-40.	23.0	20
63	Technical note: Accelerated nonrigid motionâ€compensated isotropic 3D coronary <scp>MR</scp> angiography. Medical Physics, 2018, 45, 214-222.	3.0	19
64	Machine learning in cardiovascular radiology: ESCR position statement on design requirements, quality assessment, current applications, opportunities, and challenges. European Radiology, 2021, 31, 3909-3922.	4.5	19
65	LAPNet: Non-Rigid Registration Derived in k-Space for Magnetic Resonance Imaging. IEEE Transactions on Medical Imaging, 2021, 40, 3686-3697.	8.9	19
66	Cardiac MR Motion Artefact Correction from K-space Using Deep Learning-Based Reconstruction. Lecture Notes in Computer Science, 2018, , 21-29.	1.3	18
67	Magnetic Resonance Fingerprinting Using Recurrent Neural Networks. , 2019, , .		18
68	Motion corrected water/fat wholeâ€heart coronary MR angiography with 100% respiratory efficiency. Magnetic Resonance in Medicine, 2019, 82, 732-742.	3.0	18
69	High-Resolution Self-Gated Dynamic Abdominal MRI Using Manifold Alignment. IEEE Transactions on Medical Imaging, 2017, 36, 960-971.	8.9	17
70	Multiâ€modal synergistic PET and MR reconstruction using mutually weighted quadratic priors. Magnetic Resonance in Medicine, 2019, 81, 2120-2134.	3.0	17
71	PET/MRI of atherosclerosis. Cardiovascular Diagnosis and Therapy, 2020, 10, 1120-1139.	1.7	17
72	3D Dixon water-fat LGE imaging with image navigator and compressed sensing in cardiac MRI. European Radiology, 2021, 31, 3951-3961.	4.5	17

5

#	Article	IF	CITATIONS
73	Highly efficient wholeâ€heart imaging using radial phase encodingâ€phase ordering with automatic window selection. Magnetic Resonance in Medicine, 2011, 66, 1008-1018.	3.0	16
74	Group sparse reconstruction using intensityâ€based clustering. Magnetic Resonance in Medicine, 2013, 69, 1169-1179.	3.0	16
75	Accelerated 3D T ₂ mapping with dictionaryâ€based matching for prostate imaging. Magnetic Resonance in Medicine, 2019, 81, 1795-1805.	3.0	16
76	Detection and Correction of Cardiac MRI Motion Artefacts During Reconstruction from k-space. Lecture Notes in Computer Science, 2019, , 695-703.	1.3	16
77	Compressive manifold learning: Estimating one-dimensional respiratory motion directly from undersampled k-space data. Magnetic Resonance in Medicine, 2014, 72, 1130-1140.	3.0	15
78	Simultaneous comprehensive liver T ₁ , T ₂ , , T _{1ï} , and fat fraction characterization with MR fingerprinting. Magnetic Resonance in Medicine, 2022, 87, 1980-1991.	3.0	15
79	Cardiac functional assessment without electrocardiogram using physiological selfâ€navigation. Magnetic Resonance in Medicine, 2014, 71, 942-954.	3.0	14
80	Accelerated magnetic resonance fingerprinting using soft-weighted key-hole (MRF-SOHO). PLoS ONE, 2018, 13, e0201808.	2.5	14
81	Accelerated freeâ€breathing wholeâ€heart 3D T ₂ mapping with high isotropic resolution. Magnetic Resonance in Medicine, 2020, 83, 988-1002.	3.0	14
82	High-Spatial-Resolution 3D Whole-Heart MRI T2 Mapping for Assessment of Myocarditis. Radiology, 2021, 298, 578-586.	7.3	14
83	Deep Learning Using K-Space Based Data Augmentation for Automated Cardiac MR Motion Artefact Detection. Lecture Notes in Computer Science, 2018, , 250-258.	1.3	13
84	Molecular and Nonmolecular Magnetic Resonance Coronary and Carotid Imaging. Arteriosclerosis, Thrombosis, and Vascular Biology, 2019, 39, 569-582.	2.4	13
85	Fully selfâ€gated freeâ€running 3D Cartesian cardiac CINE with isotropic wholeâ€heart coverage in less than 2 min. NMR in Biomedicine, 2021, 34, e4409.	2.8	13
86	Artificial Intelligence in Cardiac MRI: Is Clinical Adoption Forthcoming?. Frontiers in Cardiovascular Medicine, 2021, 8, 818765.	2.4	13
87	A computationally efficient OMP-based compressed sensing reconstruction for dynamic MRI. Physics in Medicine and Biology, 2011, 56, N99-N114.	3.0	12
88	3D SASHA myocardial T1 mapping with high accuracy and improved precision. Magnetic Resonance Materials in Physics, Biology, and Medicine, 2019, 32, 281-289.	2.0	12
89	Comparison of parameter optimization methods for quantitative susceptibility mapping. Magnetic Resonance in Medicine, 2021, 85, 480-494.	3.0	12
90	Prospective highâ€resolution respiratoryâ€resolved wholeâ€heart MRI for imageâ€guided cardiovascular interventions. Magnetic Resonance in Medicine, 2012, 68, 205-213.	3.0	11

#	Article	IF	CITATIONS
91	CMRA with 100% navigator efficiency with 3D self navigation and interleaved scanning. Journal of Cardiovascular Magnetic Resonance, 2014, 16, O8.	3.3	11
92	Whole left ventricular functional assessment from two minutes free breathing multi-slice CINE acquisition. Physics in Medicine and Biology, 2015, 60, N93-N107.	3.0	11
93	Accelerated 3D T ₂ wâ€imaging of the prostate with 1â€millimeter isotropic resolution in less than 3 minutes. Magnetic Resonance in Medicine, 2019, 82, 721-731.	3.0	11
94	Respiratory―and cardiac motionâ€corrected simultaneous wholeâ€heart PET and dual phase coronary MR angiography. Magnetic Resonance in Medicine, 2019, 81, 1671-1684.	3.0	11
95	3D Wholeâ€heart freeâ€breathing qBOOSTâ€T2 mapping. Magnetic Resonance in Medicine, 2020, 83, 1673-16	873.0	10
96	MRI-Guided Motion-Corrected PET Image Reconstruction for Cardiac PET/MRI. Journal of Nuclear Medicine, 2021, 62, 1768-1774.	5.0	10
97	Coronary Magnetic Resonance Angiography in Chronic Coronary Syndromes. Frontiers in Cardiovascular Medicine, 2021, 8, 682924.	2.4	10
98	High-resolution non-contrast free-breathing coronary cardiovascularÃ,Âmagnetic resonance angiography for detection of coronary artery disease: validation against invasive coronary angiography. Journal of Cardiovascular Magnetic Resonance, 2022, 24, 26.	3.3	10
99	Threeâ€dimensional late gadoliniumâ€enhanced mr imaging of the left atrium: A comparison of spiral versus Cartesian <i>k</i> â€space trajectories. Journal of Magnetic Resonance Imaging, 2014, 39, 211-216.	3.4	9
100	Simultaneous 3D wholeâ€heart brightâ€blood and black blood imaging for cardiovascular anatomy and wall assessment with interleaved T 2 prepâ€IR. Magnetic Resonance in Medicine, 2019, 82, 312-325.	3.0	8
101	3D Cartesian fast interrupted steadyâ€state (FISS) imaging. Magnetic Resonance in Medicine, 2019, 82, 1617-1630.	3.0	7
102	An MR fingerprinting approach for quantitative inhomogeneous magnetization transfer imaging. Magnetic Resonance in Medicine, 2022, 87, 220-235.	3.0	7
103	Self-supervised learning-based diffeomorphic non-rigid motion estimation for fast motion-compensated coronary MR angiography. Magnetic Resonance Imaging, 2022, 85, 10-18.	1.8	7
104	Whole-heart non-rigid motion corrected coronary MRA with autofocus virtual 3D iNAV. Magnetic Resonance Imaging, 2022, 87, 169-176.	1.8	7
105	Accelerating threeâ€dimensional molecular cardiovascular MR imaging using compressed sensing. Journal of Magnetic Resonance Imaging, 2012, 36, 1362-1371.	3.4	6
106	Weighted Manifold Alignment using Wave Kernel Signatures for Aligning Medical Image Datasets. IEEE Transactions on Pattern Analysis and Machine Intelligence, 2020, 42, 988-997.	13.9	6
107	Wholeâ€heart T 1 mapping using a 2D fat image navigator for respiratory motion compensation. Magnetic Resonance in Medicine, 2020, 83, 178-187.	3.0	6
108	Comparison of imageâ€based and reconstructionâ€based respiratory motion correction for golden radial phase encoding coronary MR angiography. Journal of Magnetic Resonance Imaging, 2015, 42, 964-971.	3.4	5

#	Article	IF	CITATIONS
109	Space-time variant weighted regularization in compressed sensing cardiac cine MRI. Magnetic Resonance Imaging, 2019, 58, 44-55.	1.8	5
110	Current Applications and Future Development of Magnetic Resonance Fingerprinting in Diagnosis, Characterization, and Response Monitoring in Cancer. Cancers, 2021, 13, 4742.	3.7	5
111	Non-rigid motion-corrected free-breathing 3D myocardial Dixon LGE imaging in a clinical setting. European Radiology, 2022, 32, 4340-4351.	4.5	5
112	SIRF: Synergistic Image Reconstruction Framework. , 2017, , .		4
113	Accelerated high-resolution free-breathing 3D whole-heart T2-prepared black-blood and bright-blood cardiovascular magnetic resonance. Journal of Cardiovascular Magnetic Resonance, 2020, 22, 88.	3.3	4
114	Motionâ€corrected and highâ€resolution anatomically assisted (MOCHA) reconstruction of arterial spin labeling MRI. Magnetic Resonance in Medicine, 2020, 84, 1306-1320.	3.0	4
115	Contrast-free high-resolution 3D magnetization transfer imaging for simultaneous myocardial scar and cardiac vein visualization. Magnetic Resonance Materials in Physics, Biology, and Medicine, 2020, 33, 627-640.	2.0	4
116	Faster 3D saturation-recovery based myocardial T1 mapping using a reduced number of saturation points and denoising. PLoS ONE, 2020, 15, e0221071.	2.5	4
117	Channel Attention Networks for Robust MR Fingerprint Matching. IEEE Transactions on Biomedical Engineering, 2022, 69, 1398-1405.	4.2	4
118	3D whole-heart grey-blood late gadolinium enhancement cardiovascular magnetic resonance imaging. Journal of Cardiovascular Magnetic Resonance, 2021, 23, 62.	3.3	4
119	Synergistic multi-contrast cardiac magnetic resonance image reconstruction. Philosophical Transactions Series A, Mathematical, Physical, and Engineering Sciences, 2021, 379, 20200197.	3.4	4
120	Evaluation of accelerated motion-compensated 3d water/fat late gadolinium enhanced MR for atrial wall imaging. Magnetic Resonance Materials in Physics, Biology, and Medicine, 2021, 34, 877-887.	2.0	4
121	Efficient non-contrast enhanced 3D Cartesian cardiovascular magnetic resonance angiography of the thoracic aorta in 3Âmin. Journal of Cardiovascular Magnetic Resonance, 2022, 24, 5.	3.3	4
122	Accelerating 3D MTC-BOOST in patients with congenital heart disease using a joint multi-scale variational neural network reconstruction. Magnetic Resonance Imaging, 2022, 92, 120-132.	1.8	4
123	TRIO a Technique for Reconstruction Using Intensity Order: Application to Undersampled MRI. IEEE Transactions on Medical Imaging, 2011, 30, 1566-1576.	8.9	3
124	MRI slice stacking using manifold alignment and wave kernel signatures. , 2018, , .		3
125	A Spatial Off-Resonance Correction in Spirals for Magnetic Resonance Fingerprinting. IEEE Transactions on Medical Imaging, 2021, 40, 3832-3842.	8.9	3
126	Quality-Aware Cine Cardiac MRI Reconstruction andÂAnalysis fromÂUndersampled K-Space Data. Lecture Notes in Computer Science, 2022, , 12-20.	1.3	3

#	Article	IF	CITATIONS
127	A 3D MR-acquisition scheme for non-rigid bulk motion correction in simultaneous PET-MR. EJNMMI Physics, 2014, 1, A37.	2.7	2
128	Evaluation of Strategies for PET Motion Correction - Manifold Learning vs. Deep Learning. Lecture Notes in Computer Science, 2018, , 61-69.	1.3	2
129	Dynamic Volume Reconstruction from Multi-slice Abdominal MRI Using Manifold Alignment. Lecture Notes in Computer Science, 2016, , 493-501.	1.3	2
130	Innovations in Cardiovascular MR and PET-MR Imaging. , 2022, , 265-309.		2
131	Calcium (Ca2+) waves data calibration and analysis using image processing techniques. BMC Bioinformatics, 2013, 14, 162.	2.6	1
132	Accelerating dual cardiac phase images using undersampled radial phase encoding trajectories. Magnetic Resonance Imaging, 2016, 34, 1017-1025.	1.8	1
133	Efficient Deformable Motion Correction for 3-D Abdominal MRI Using Manifold Regression. Lecture Notes in Computer Science, 2017, , 270-278.	1.3	1
134	PET-MR respiratory signal estimation using semi-supervised manifold alignment. , 2018, , .		1
135	Quantitative magnetization transfer imaging for nonâ€contrast enhanced detection of myocardial fibrosis. Magnetic Resonance in Medicine, 2021, 85, 2069-2083.	3.0	1
136	Whole-Heart Single Breath-Hold Cardiac Cine: A Robust Motion-Compensated Compressed Sensing Reconstruction Method. Lecture Notes in Computer Science, 2017, , 58-69.	1.3	1
137	Accelerated 4D Respiratory Motion-Resolved Cardiac MRI with a Model-Based Variational Network. Lecture Notes in Computer Science, 2020, , 427-435.	1.3	1
138	Magnetization Transfer <scp>BOOST</scp> Noncontrast Angiography Improves Pulmonary Vein Imaging in Adults With Congenital Heart Disease. Journal of Magnetic Resonance Imaging, 0, , .	3.4	1
139	A New Method to Quantify Aortic Biomechanics In Vivo Using Four-Dimensional Magnetic Resonance Imaging (4D MRI): Implications for Ascending Aortic Endografts. Journal of Vascular Surgery, 2013, 57, 20S.	1.1	0
140	Multiresolution reconstruction of real-time MRI with motion compensated compressed sensing: Application to 2D free-breathing cardiac MRI. , 2016, , .		0
141	Highly efficient motion-corrected simultaneous cardiac PET-MR imaging. , 2016, , .		0
142	Multi-modal weighted quadratic priors for robust intensity independent synergistic PET-MR reconstruction. , 2017, , .		0
143	Cardiac MR Angiography. , 2018, , 399-432.		0
144	Thrombosis and Embolism. , 2021, , 1225-1244.		0

Claudia Prieto

#	Article	IF	CITATIONS
145	Elastic AlignedSENSE for Dynamic MR Reconstruction: A Proof of Concept in Cardiac Cine. Entropy, 2021, 23, 555.	2.2	0
146	Technical Advances and Clinical Perspectives in Coronary MR Imaging. , 2018, , 321-344.		0
147	Atherosclerotic Plaque Imaging. , 2019, , 343-351.e3.		0
148	Magnetic Resonance Imaging of Coronary Arteries. , 2019, , 291-299.e5.		0
149	Specialized Mapping Methods in the Heart. Advances in Magnetic Resonance Technology and Applications, 2020, 1, 91-121.	0.1	0
150	Motion Estimation Applied to Reconstruct Undersampled Dynamic MRI. , 2007, , 522-532.		0